Astron. Astrophys. 322, 427–430 (1997)

ASTRONOMY
AND
ASTROPHYSICS

CO emission from 3C 48

J.E. Wink[1], **S. Guilloteau**[1], **and T.L. Wilson**[2,3]

[1] IRAM, 300 Rue de la Piscine, F-38406 St. Martin d'Hères, France
[2] Max-Planck-Institut für Radioastronomie, Auf dem Hügel 69, D-53121 Bonn, Germany
[3] Astronomy Dept., University of Illinois, 1002 W. Green St., Urbana, Ill., 61801 USA

Received 17 October 1996 / Accepted 2 December 1996

Abstract. The measurement of the J=1–0 line of CO with the IRAM interferometer is reported. The CO line parameters are in good agreement with the result given by Scoville et al. (1993). Thus, CO emission from 3C 48, a radio loud QSO, is definitely detected. The CO emission region is marginally resolved. Source parameters based on the CO line data are discussed.

Key words: radio lines: galaxies – quasars: 3C 48 – galaxies: ISM

1. Introduction

The source 3C 48 is of special interest since this was one of the first quasi stellar radio sources (hereafter QSO's) found, and also one of the first QSO's found to be associated with a galaxy (Sandage & Miller 1966; Boronson & Oke 1982). Furthermore, the galaxy is the brightest of any observed thus far (Neugebauer et al. 1985), and this object shows signs of a tidal interaction (Gehren et al. 1984), as well as a double nucleus with a radio jet (Wilkinson et al. 1991). These data indicate a possible merger, as well as a link between radio loud QSO's and galaxy mergers (see, e.g., the discussion of Sanders et al. 1988). For all of these reasons, it is of great interest to obtain an estimate of the gas mass and to determine the relative position of the molecular gas relative to the continuum emission. Scoville et al. (1993) reported a 4 σ detection of emission from the J= $1-0$ line of CO. In view of the importance of this result, we were convinced that a prolonged search, as well as a higher resolution image of the CO emission was of high importance.

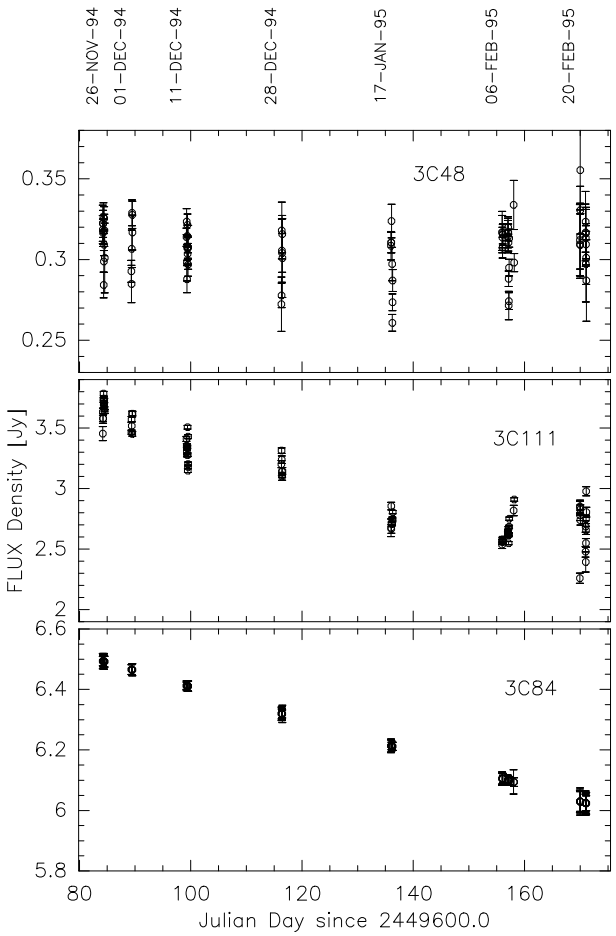

Fig. 1. The flux densities of the three sources as function of time

2. Observations and data reduction

The observations were performed with the IRAM Interferometer on Plateau de Bure (Guilloteau et al. 1992) in BC configuration between 26 Nov 1994 and 08 Feb 1995 with 4 antennas and 20 and 21 Feb 1995 with 3 antennas. Since we were searching for a small percentage of the continuum signal any success would depend on the accuracy of frequency bandpass calibration. Therefore, we observed using a basic observing cycle of 5 min on 3C 84, 10 min on 3C 48, and 5 min on 3C 111. Using the data taken from 3C 84, we searched for instrumental variations in the frequency baselines as function of time. We frequently focussed and pointed on 3C 84 or 3C 111 to maintain optimal values. The SIS receivers were single sideband

Send offprint requests to: J.E. Wink

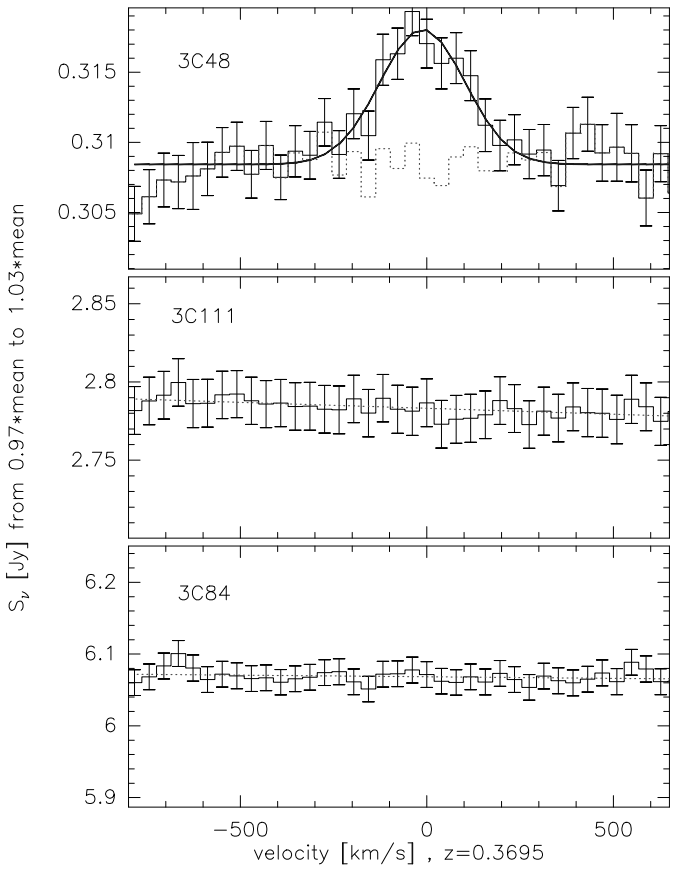

Fig. 2. In the topmost panel, we present our spectrum of 3C 48, shown as a histogram, together with the gaussian fit to the data, shown as a smooth line. In the middle and lower panels are shown our spectra of 3C 111 and 3C 84. Each panel spans ±3% around the mean flux to demonstrate the quality of the instrumental baseline.

tuned to 84.17 GHz with a typical upper sideband rejection of 6 dB. Typical receiver temperatures were 50 K. 6 correlator units were used with 2.5 MHz wide channels. The number of channels evaluated was 180 , the total bandwidth used was 450 MHz. The weather was in general favourable with about 3 mm of water vapour. Telescope spacings ranged from 24 to 288 m. The resulting half power beam sizes using uniform weighting are 4.33 x 1.79 ″at position angle 34° for 3C 48, 3.84 x 2.15 ″at position angle 50° for 3C 84, and 3.92 x 2.17 ″at position angle 56° for 3C 111.

The observations were reduced with the CLIC and GILDAS reduction packages developed at IRAM and Observatory of Grenoble. The frequency bandpass was calibrated for each observing night by fitting a polynomial through the data for 3C 84 and applying it for all sources. We noticed variations in the slope of the bandpass with elevation of up to 2° and 0.3 % on antenna #2. This was traced to a backshort in the receiver slipping at high elevation. Since the three sources were at different elevation, this effect could not be completely compensated. The effect is expected to be more than an order of magnitude less, when combining the data from different baselines and configurations.

In the reduction process we noted variation of the flux ratio 3C 84/3C 111. As 3C 48 is one of the prime calibrators used by observers at the Very Large Array, we used it to calibrate amplitudes and phases as function of time. The flux density was originally fixed at 307 mJy. From comparisons with W3(OH), which was measured at the end of each observing session and for which we assumed a flux density at 84.17 GHz of 3.7 Jy, we obtained 294 ± 10 mJy. In Fig.1 we plot the flux densities of these three sources as a function of time. These results are measured relative to 3C 84; the flux density of this source has decreased by 6 % and that of 3C 111 by 31 % . In this intensity scale the flux density for 3C 48 is 307 ± 1.5 mJy. Comparisons with measurements of 3C 84 based on planets at the 30-m show our intensity scale is accurate to about 5%.

We then binned the data into 11 MHz (38 km s^{-1}) wide channels to produce maps. The amplitudes from the fit of a circular Gaussian to the visibility data are shown in Fig.2, together with linear fits for 3C 84 and 3C 111 and a Gaussian fit for 3C 48. The slope for 3C 84 is 7.3 10^{-7} and that for 3C 111 is 2.7 10^{-6} in agreement with the flat spectral index of 3C 111 as opposed to the steeper slope of 3C 84. The intensity scale was fixed to ±3 % around the mean flux in each case to make the spectra compatible. One still can see some systematic effects such as those at velocities below -650 km s^{-1}and the low channel at -160 km s^{-1}; these channels are at the edge of the subbands and where we had no overlap. Their effect is below the 1 % level. The CO line in 3C 48 is detected with a signal-to-noise ratio of 6 to 1 at the line maximum. Taking the FWHP linewidth and our velocity resolution into account, we have 6 independent data points above half power, so that this line is detected with a signal-to-noise ratio of 9 to 1. However, systematic effects must also be considered, and our (expected) negative results for the more intense sources 3C 84 and 3C 111 demonstrate that this detection is reliable. The gaussian fit gives a continuum of 308 ± 1 mJy, a peak line emission of 9 ± 1 mJy, a line half power width of 260 ± 30 km s^{-1}centered at 12 ± 10 km s^{-1} in the z=0.3695 reference system. These parameters are listed in Table 1 together with other data derived below.

Fig.3 shows the cleaned map produced for 3C 48 after self-calibration and applying a gaussian taper to the visibility data and after subtracting a point source, the continuum, from the visibility data. The CO emission is found to be close to the phase center.

To study the size of the CO emission region we fitted elliptical and circular Gaussians to the visibility data. The results change slightly whether we subtract the corner channels for the continuum or whether we subtract a constant from the real part of the visibility. This second method gives somewhat lower noise. This is not surprising, since the second method adds no noise to the visibilities. In the following we show the spectral line distribution resulting when we subtract a constant from the real part of the visibility, but we consider the first approach in the error estimate. Fig.4 shows the result of the circular fit. From bottom to top are the flux density, the offset in Right Ascension, the offset in Declination, and the half power size. The upper panel indicates the CO emitting region to be extended: 1

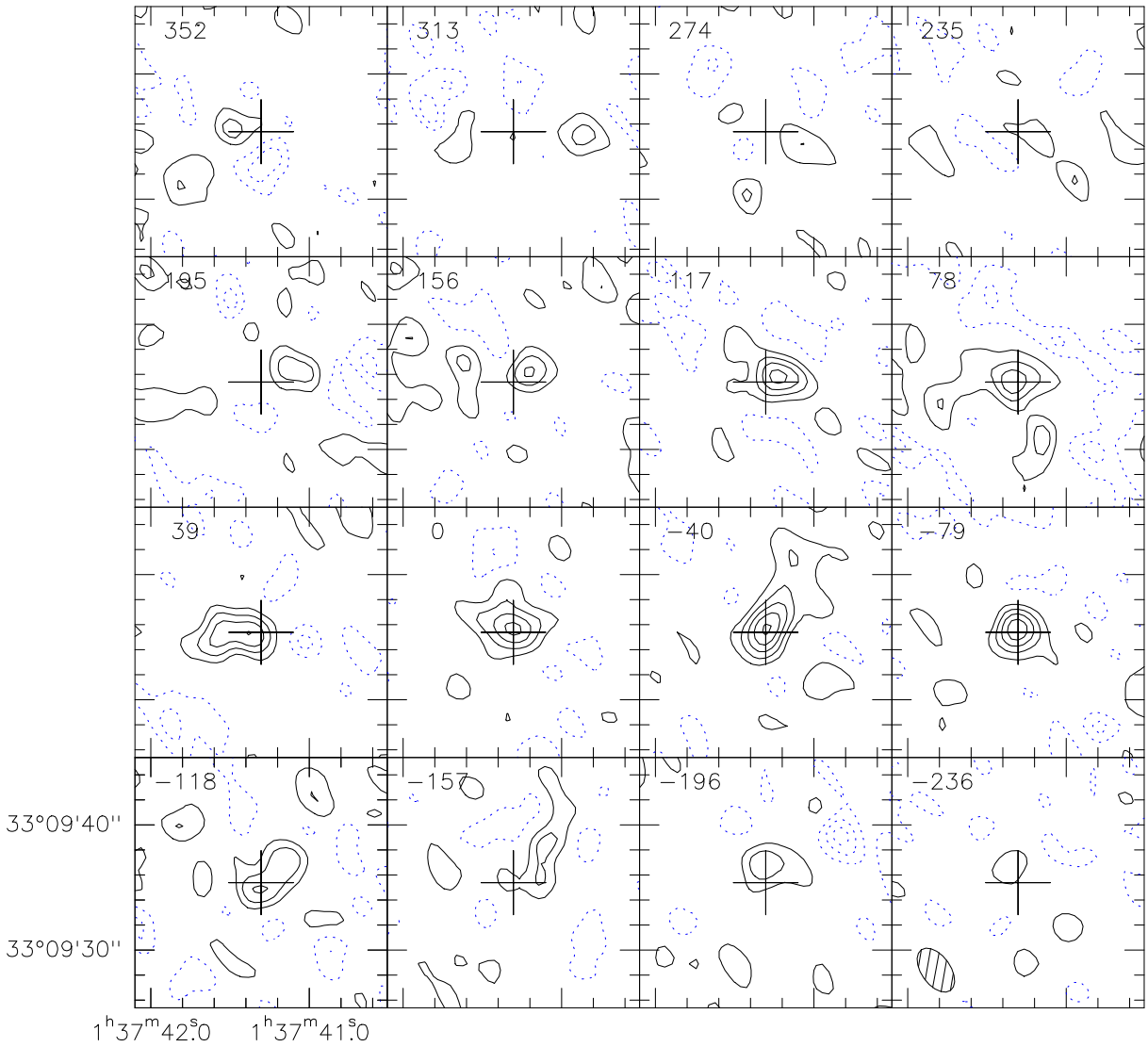

Fig. 3. The channel maps after subtracting the channels for velocities -500 to -800 and 500 to 700 km s^{-1}from the visibilities using a gaussian taper of 200m. The clean beam of 4 x 2.3 ″at position angle 35° is shown as dashed ellipse in the lower right panel. Contour levels are at -6, -4, -2, 2, 4, 6, 8, 10 mJy/beam (1 Jy/beam = 20.6 K)

to 1.5″(1.30±0.23″ for the average of 7 channels). Note that, since we used self-calibration, this value is not affected by seeing effects. We also tried to fit an elliptical gaussian to the visibility data. The elliptical fits did however not converge, not surprising in view of fitting two more parameters to noisy data.

We consider the possible chance coincidence of finding CO along the line of sight to 3C 48. If this were the case we might expect to find absorption against 3C 48. Therefore we also made a combined spectrum with the full resolution of 2.5 MHz (= 9km s^{-1}). Any absorption is less than 3%.

3. Results and comparison with earlier work

1. A comparison of our result with that of Scoville et al. (1993) shows excellent agreement of the line parameters, although our continuum flux is 16 % larger than that given by Scoville et al. (1993). As quoted above, our flux density scale is based on the comparison with W3(OH), which we had to correct for resolution, but our absolute scale is in agreement with measurements of 3C 84 based on planets.

2. We used two methods to deconvolve our beam. The first is to subtract the average of velocity channels between 400 to 700 and -800 to -500 km s^{-1} from the (u,v) plane data. This gives a FHWP size for the CO data of 1.6″. The second method is to subtract a constant (the continuum) from the real part in the (u,v) plane data. This gives a size of 1.3″ for the CO emission. From the velocity channels displayed in Fig. 3, there is a variation in position in R.A. but not in Dec. These data may indicate that the CO emission is extended at right angles to the direction of the VLBI jet (Wilkinson et al. 1991), but this result is highly speculative because of the signal-to-noise ratio. For

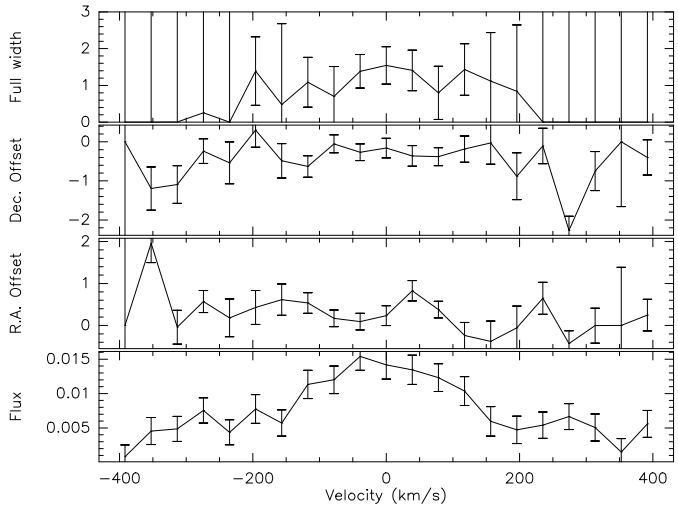

Fig. 4. The amplitudes, position offsets and full half power widths of the continuum subtracted CO visibilities.

Table 1. Observed and derived parameters for 3C 48

continuum S_ν	(Fig 1-2)	307 ± 1.5 mJy
continuum size		$< 1''$
line strength	(Fig.2)	9.0 ± 1.5 mJy
line center	(Fig.2)	z = .36948
line width FWHP	(Fig.2)	270 ± 20 km s^{-1}
$S_{CO}\Delta V(1 \rightarrow 0)$		2.4 ± 0.4 Jy·km s^{-1}
L'$_{CO}$		$2.7 \cdot 10^9$ L$_\odot$
angular extent FWHP		$1.30 \pm 0.23\,''$
for H_0 = 75km s^{-1}Mpc^{-1}, q_0 = 0.5		
luminosity distance		1.6 Gpc
angular size distance		849 Mpc
linear mean diameter		6 ± 2 kpc
dynamical mass		$5 \pm 1\ 10^{10}$ M$_\odot$
$S_{CO}\Delta V/S_{100(1+z)}$		2.5 km s^{-1}

H_0 = 75km s^{-1}Mpc^{-1}, q_0 = 0.5, the angular distance for the redshift of 0.3695 is 849 Mpc; therefore, the true (deconvolved) size ranges from 5 to 7 kpc. This size is nearly the diameter of the molecular ring in our own galaxy. In Table 1 we have combined the observed and reduced data. (We use the designations and formulae as given by Solomon et al. 1992).

3. We combine the FWHP linewidth and source radius to estimate the dynamical mass. This is

$$\mathrm{M}_{dyn} = 232 \cdot \frac{R}{[\mathrm{pc}]} \cdot (\frac{v}{[\mathrm{km\ s^{-1}}]})^2$$

i.e. 5 10^{10} M$_\odot$. This must be considered as a lower limit, since we use the mean radius and do not correct for inclination. However, this dymamical mass approaches the typical value for a large galaxy, e.g. the Milky Way (Dame 1992 and references therein).

4. Any further interpretation of this data requires a number of assumptions, since only one molecular line has been detected. The integrated CO line flux is 2.4 ± 0.4 Jy·km s^{-1}. Using the standard conversion of integrated CO intensity to H_2 masses we obtain $M_{H_2} = 2.7 \cdot 10^{10}\,\mathrm{M}_\odot$. This is 50 % of the dynamical mass, which includes the mass in stars, a relatively high ratio. But first, as shown above, the actual dynamical mass will be larger and second the H_2 mass to L'$_{CO}$ conversion factor may be lower than the 4.6 M$_\odot$ (K·km s^{-1}·pc^2) $^{-1}$, since there are many galaxies for which the ratio of the gas mass derived from CO to the dynamical mass is $\sim$ 75%. (e.g. Solomon et al.1990)

5. There are a number of objects showing CO emission, with redshifts which are of order 0.1. Our mass estimate for 3C 48 is three times that of Arp 220, comparable to Mrk 1014 but somewhat larger than IRAS 14349-1447. If we take the IR data of Neugebauer et al. (1985), we obtain a luminosity to H_2 mass ratio of 40 L$_\odot$ M$_\odot^{-1}$, which is one-half that obtained for Arp 220.

4. Conclusions

From our measurements of the J=1-0 line of CO with the IRAM interferometer, we conclude that:
(1) The detection of CO in 3C 48 and the line parameters of Scoville et al. (1993) are confirmed.
(2) With our better angular resolution and sensitivity, we find that the CO emission is extended over $1''$ to $1.5''$.
(3) From the angular size, distance and linewidth, we find a virial mass of 5 10^{10} M$_\odot$. This is comparable to the mass of the Milky Way within a galactocentric distance of 5 kpc.
(4) From a comparison of the "CO mass" with the virial mass we find that the CO to H_2 conversion factor is $\sim$5.6 if the virial mass refers only to the H_2 mass.

Acknowledgements. We thank D. Downes for helpful discussions and the anonymous referee for his comments. During a portion of this work, TLW was supported by a G.A. Miller professorship at the Univ. of Illinois. He also thanks L. E. Snyder for hospitality while in Urbana.

References

Boronson T.A., Oke J.B., 1982 Nature 296, 397
Dame T.M. in 'Back to the Galaxy', eds. S.S.Holt and F.Verter, Am. Inst. of Physics, New York 1993
Gehren T., Fried J., Wehinger P.A., Wyckoff S., 1984 ApJ 278, 11
Guilloteau S., Delannoy J., Downes D., et al. 1992 A&A 262, 624
Neugebauer G., Soifer B.T., Miley G.K. 1985 ApJ 295, L27
Sandage A.R., Miller W.C. 1966 ApJ 144, 1266
Sanders D.B., Soifer B.T., Elias J.H., Madore B.F., Matthews K., Neugebauer G., Scoville N.Z. 1988, ApJ 325, 74
Scoville N.Z., Padin S., Sanders D.B., Soifer B.T., Yun M.S. 1993 ApJ 415, L75
Solomon P.M., Radford S.J.E., Downes D. 1990 ApJ 348, L53
Solomon P.M., Radford S.J.E., Downes D. 1992 Nature 356, 318
Wilkinson P.N., Tzoumis A.K., Benson J.M., Walker R.C., Simon R.S., Kahn F.D. 1991 Nature 352, 313

This article was processed by the author using Springer-Verlag LaTeX A&A style file *L-AA* version 3.